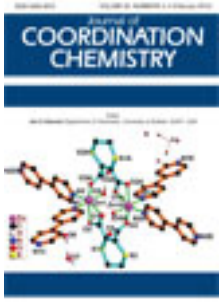

Journal of Coordination Chemistry
Publication details, including instructions for authors and subscription information:
http://www.tandfonline.com/loi/gcoo20

Synthesis and characterization of 4,4′-methylenebis (2,6-di-tert-butylphenol) derivatives of a series of metal alkoxides and alkyls

Timothy J. Boyle [a] , Leigh Anna M. Steele [a] & Daniel T. Yonemoto [a]
[a] Sandia National Laboratories, Advanced Materials Laboratory , 1001 University Boulevard, SE , Albuquerque , NM 87106 , USA
Published online: 30 Jan 2012.

To cite this article: Timothy J. Boyle , Leigh Anna M. Steele & Daniel T. Yonemoto (2012) Synthesis and characterization of 4,4′-methylenebis (2,6-di-tert-butylphenol) derivatives of a series of metal alkoxides and alkyls, Journal of Coordination Chemistry, 65:3, 487-505, DOI: 10.1080/00958972.2012.654785

To link to this article: http://dx.doi.org/10.1080/00958972.2012.654785

Journal of Coordination Chemistry
Vol. 65, No. 3, 10 February 2012, 487–505

Synthesis and characterization of 4,4′-methylenebis (2,6-di-*tert*-butylphenol) derivatives of a series of metal alkoxides and alkyls

TIMOTHY J. BOYLE*, LEIGH ANNA M. STEELE and DANIEL T. YONEMOTO

Sandia National Laboratories, Advanced Materials Laboratory, 1001 University Boulevard, SE, Albuquerque, NM 87106, USA

(*Received 27 October 2011; in final form 6 December 2011*)

Investigation of the coordination behavior of 4,4′-methylenebis(2,6-di-*tert*-butylphenol) (or H_2-4DBP) with a series of metal alkoxides led to isolation of $[(OR)_3M]_2(\mu\text{-4DBP})$, where M/OR = Ti/OBu^t (**2**), Ti/ONep (**3**), Zr/OBu^t (**4**), Hf/OBu^t (**5**), and $[(py)(OR)_3M]_2(\mu\text{-4DBP})\cdot py$ (**5a**), where py = pyridine and ONep = $OCH_2C(CH_3)_3$. Metal alkyl derivatives of 4DBP were also studied and found to form similar di-substituted species: $[(py)_2(Et)Zn]_2(\mu\text{-4DBP})\cdot py$ (**6**), $[(THF)_3(Br)Mg]_2(\mu\text{-4DBP})$ (**7**), $[(THF)_2(Br)Mg](\mu\text{-4DBP})[Mg(Br)(THF)_3]\cdot$(THF, tol) (**7a**), and $[(py)(R)_2Al]_2(\mu\text{-4DBP})$, where R = CH_3 (**8**), Et (**9**), $CH_2CH(CH_3)_2$ (**10**); tol = toluene and THF = tetrahydrofuran. All structures demonstrate the bridging nature of 4DBP and the ability to bind a variety of metal centers. Solution state NMR indicates that the structures of **2**–**10** are retained in solution. Thermal analyses indicate that 4DBP is preferentially lost during heating.

Keywords: Metal alkoxides; Bidentate phenoxides; Group 4; Aluminum; Zinc; Magnesium

1. Introduction

Metal alkoxides $[M(OR)_x]$ have found widespread utility as precursors to ceramic oxide materials in bulk powder, thin film, or nanomaterial form. In many instances, the nuclearity of the $M(OR)_x$ precursor has been shown to play a role in determining the various properties of the final ceramic [1–13]; therefore, it is of interest to garner control over the structure of these precursors. Unfortunately, due to the large cation size and small charge of the ligands, $M(OR)_x$ often suffer from clustering and oligomerization with bridging alkoxide (μ-OR) ligands filling open coordination sites. We have demonstrated some control of the assembly of $Ti(OR)_4$ using select ligands, such as dihydroxypyridimine (H_2-DHP) [14] and pyridine carbinol (H–OPy) [15] shown in figure 1(a) and (b). Previously, the DHP ligand was found to act solely as a bridging ligand between "$Ti(OR)_3$" moieties but the solubility of the resulting complex was significantly reduced. For the OPy derivatives, two ligands preferentially bind bidentate

*Corresponding author. Email: tjboyle@Sandia.gov

ISSN 0095-8972 print/ISSN 1029-0389 online
http://dx.doi.org/10.1080/00958972.2012.654785

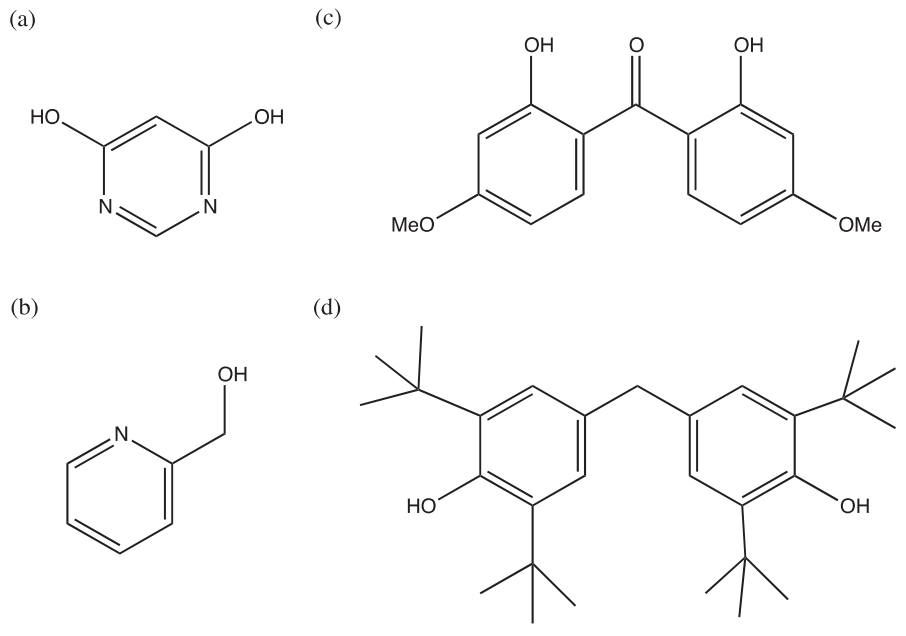

Figure 1. Schematic representation of polydentate ligands (a) dihydroxypyridimine (H_2-DHP), (b) pyridine carbinol (H-OPy), (c) 4,4′-di-methoxy,2,2′-di-ol-benzophenone (H_2-OBzP), and (d) 4,4′-methylenebis(2,6-di-*tert*-butylphenol) (H_2-4DBP).

to the Ti cation, thereby directing alcoholysis reactions to the remaining alkoxide ligands [15].

Continuing our efforts to generate controlled structures of $M(OR)_x$, we have undertaken an investigation of polydentate aryloxide (OAr) ligands. These ligands were of particular interest due to our previous success with aryl alcohol (phenols) [16–22] and catechol [22] ligands in generating complex families of $M(OR)_x$ compounds. Since we had already explored polyhydroxide aryl rings with the catechol species, it was thought that if the aryl rings were linked, the OH positioning would facilitate control over the final structures. This proved a valuable approach for generating dinuclear species when using the 4,4′-di-methoxy,2,2′-di-ol-benzophenone (H_2-OBzP) (figure 1c) [23]. For OBzP, the rigid aryl backbone and C=O moiety led to a close interaction of two metals [23].

For this study, the coordination behavior of the underexplored 4,4′-methylenebis(2,6-di-*tert*-butylphenol) (referred to as H_2-4DBP or **1**) ligand was undertaken. The schematic structure of **1** is shown in figure 1(d) and a thermal plot in figure 2. The ligand possesses more flexibility in comparison to OBzP or catecholate derivatives and the *para*-OH make it of interest for controlled alcoholysis. Following equations (1) and (2), the structural influence introduced by these ligands was determined for a series of $M(OR)_x$ and metal alkyls (MR_x), respectively.

$$2M(OR)_4 + H_2\text{-}4DBP \longrightarrow \left[(OR)_3M\right]_2(\mu\text{-}4DBP) + 2HOR \qquad M = Ti, Zr, Hf \tag{1}$$

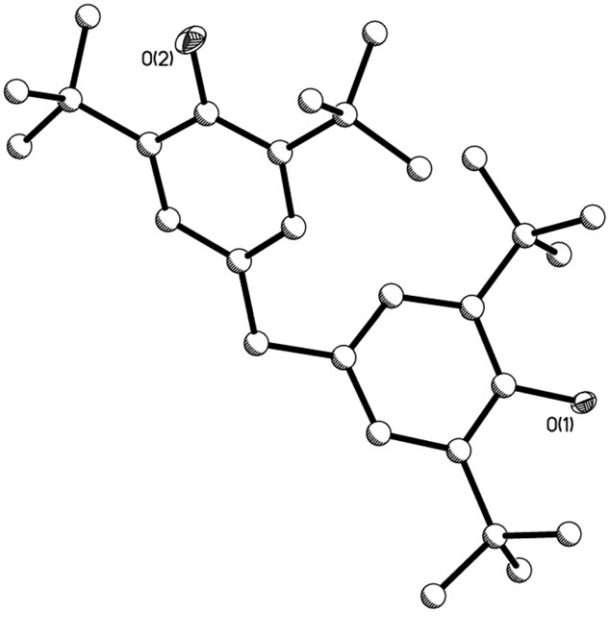

Figure 2. Structure plot of **1**. Heavy atom thermal ellipsoids drawn at 30% level and carbon atoms drawn as ball and stick for simplicity.

$$2M(R)_x + H_2\text{-}4DBP \xrightarrow{py} \left[(py)_n(R)_{x-1}M\right]_2(\mu\text{-}4DBP) + 2HR$$
$$x = 2:\ M = Zn, Mg;\ \ x = 3:\ M = Al. \tag{2}$$

The products isolated were characterized by single-crystal X-ray diffraction and identified as $[(OR)_3M]_2(\mu\text{-}4DBP)]$, where $M/OR = Ti/OBu^t$ (**2**), Ti/ONep (**3**), Zr/OBu^t (**4**), Hf/OBu^t (**5**), and $[(py)(OR)_3M]_2(\mu\text{-}4DBP)\cdot py$ (**5a**), where $OBu^t = OC(CH_3)_3$, $ONep = OCH_2C(CH_3)_3$ and py = pyridine. Investigation of metal alkyl structures that employ 4DBP led to isolation of $[(py)_2(Et)Zn]_2(\mu\text{-}4DBP)\cdot py$ (**6**, $Et = CH_2CH_3$), $[(THF)_3(Br)Mg]_2(\mu\text{-}4DBP)$ (**7**), $[(THF)_2(Br)Mg](\mu\text{-}4DBP)[Mg(Br)(THF)_3]\cdot(THF,tol)$ (**7a**), and $[(py)(R)_2Al]_2(\mu\text{-}4DBP)$, where $R = CH_3$ (**8**), Et (**9**), $CH_2CH(CH_3)_2$ (**10**), tol = toluene. The synthesis and characterization of these compounds and comparison to appropriate literature compounds will be discussed.

2. Experimental

2.1. *Materials and methods*

All compounds described below were handled with rigorous exclusion of air and water using standard Schlenk line and glovebox (argon) techniques. All solvents were stored under argon and used as received (Aldrich) in Sure/Seal^{TM} bottles, including toluene, tetrahydrofuran, and pyridine. The following chemicals were used as received (Aldrich

and Alfa Aesar): H_2-4DBP, H–ONep, $Ti(OPr^i)_4$, $M(OBu^t)_4$ (M = Ti, Zr, Hf), AlR_3 (R = Me, Et, Bu^i), $ZnEt_2$ (1 M in hexanes), and (Mes)MgBr (1 M in THF). $[Ti(\mu\text{-ONep})(ONep)_3]_2$ was prepared according to literature procedures [24].

FTIR data were collected on a Nicolet 6700 FTIR spectrometer using a KBr pellet press under a flowing nitrogen atmosphere. Elemental analysis was performed on a Perkin-Elmer 2400 CHN-S/O Elemental Analyzer. Thermal gravimetric analyses were conducted using a Mettler Toledo, TGA/DSC 1, STAR^e System under a flowing argon atmosphere from room temperature to 650°C at 5°C min^{-1}. Melting points were determined using an Electrothermal® Melting Point Apparatus from room temperature to 300°C. All NMR samples were prepared from dried crystalline materials that were handled and stored under an argon atmosphere and redissolved in toluene-d_8 or pyridine-d_5.

2.2. *Alkoxide general synthesis*

Due to the similarity of synthesis of **2**–**5**, a general description is supplied for this set of compounds. One equivalent of H_2-4DBP was slowly added to a stirring solution of two equivalents of $M(OR)_4$ dissolved in toluene (~5 mL). For each reaction the colorless reaction mixture immediately turned bright yellow. After stirring for 12 h, if the reaction was cloudy it was warmed slightly until all material was re-dissolved. All solutions were left at room temperature with slow evaporation of any volatile components, until crystals formed. Yields were not optimized and are reported for the first batch of crystals isolated.

2.2.1. $[(OBu^t)_3Ti]_2(\mu$-4DBP) (2). Used $Ti(OBu^t)_4$ (1.00 g, 2.94 mmol) and H_2-4DBP (0.624 g, 1.47 mmol). Yield: 1.29 g (46.0%). FTIR (KBr, cm^{-1}): 3068 (w), 3007 (m), 2971 (s), 2870 (s), 2707 (w), 1458 (w), 1419 (s), 1390 (w), 1361 (s), 1263 (s,sh), 1199 (s), 1124 (m), 1043 (s), 999 (s), 882 (s), 853 (w), 795 (m), 774 (w), 701 (w), 591 (m), 482(w). ^{1}H NMR (400.1 MHz, tol-d_8) δ 7.23 (1.8H, s, $[OC_6H_2(C(CH_3)_3)_2]_2CH_2$), 3.94 (1.0H, s, $[OC_6H_2(C(CH_3)_3)_2]_2CH_2$), 1.61 (18.3H, s, $[OC_6H_2(C(CH_3)_3)_2]_2CH_2$), 1.33 (27.0H, s, $OC(CH_3)_3$). Anal. Calcd for $C_{53}H_{96}O_8Ti_2$ (%): C, 66.51; H, 10.11. Found: C, 66.26; H, 10.41.

2.2.2. $[(ONep)_3Ti]_2(\mu$-4DBP) (3). Used $Ti(ONep)_4$ (0.500 g, 1.26 mmol) and H_2-4DBP (0.268 g, 0.631 mmol). Yield: 0.545 g (41.6%). FTIR (KBr, cm^{-1}): 3070 (w), 2998 (m,sh), 2954 (s), 2909 (s), 2867 (s), 2851 (s,sh), 2782 (w,sh), 2744 (w), 2698 (w), 1478 (m), 1465 (m), 1420 (s), 1394 (m), 1361 (m), 1623 (s,sh), 1246 (s), 1215 (w), 1144 (s), 1087 (s), 1025 (s), 935 (w), 892 (s), 864 (w,sh), 707 (s), 673 (s), 609 (w), 482 (w). ^{1}H NMR (400.1 MHz, tol-d_8) δ 7.27 (2H, s, $[OC_6H_2(C(CH_3)_3)_2]_2CH_2$), 4.12 (6H, s, $OCH_2C(CH_3)_3$), 3.99 (0.9H, s, $[OC_6H_2(C(CH_3)_3)_2]_2CH_2$), 1.63 (19H, s, $[OC_6H_2(C(CH_3)_3)_2]_2CH_2$), 0.96 (27H, s, $OCH_2C(CH_3)_3$). Anal. Calcd for $C_{59}H_{108}O_8Ti_2$ (%): C, 68.06; H, 10.45. Found: C, 67.38; H, 10.68.

2.2.3. $[(OBu^t)_3Zr]_2(\mu$-4DBP) (4). Used $Zr(OBu^t)_4$ (1.00 g, 2.60 mmol) and H_2-4DBP (0.553 g, 1.30 mmol). Yield: 1.50 g (55.4%). FTIR (KBr, cm^{-1}): 3068 (w), 2970 (s), 2926 (s,sh), 2869 (s), 1469 (m), 1422 (s), 1389 (m), 1359 (s), 1256 (s), 1232 (s), 1206 (s), 1123

(m), 1040 (s), 1001 (s), 921 (w), 894 (m), 867 (s), 786 (s), 750 (w), 697 (m), 627 (w), 595 (m), 553 (m), 486 (m). ^{1}H NMR (400.1 MHz, tol-d$_8$) δ 7.27 (2.0H, s, [OC$_6$*H*$_2$(C(CH$_3$)$_3$)$_2$]$_2$CH$_2$), 4.01 (1.0H, s, [OC$_6$H$_2$(C(CH$_3$)$_3$)$_2$]$_2$C*H*$_2$), 1.57 (16.7H, s, [OC$_6$H$_2$(C(C*H*$_3$)$_3$)$_2$]$_2$CH$_2$), 1.31 (27.0 H, s, OC(C*H*$_3$)$_3$). Anal. Calcd for C$_{53}$H$_{96}$O$_8$Zr$_2$ (%): C, 60.99; H, 9.27. Found: C, 60.96; H, 9.09.

2.2.4. [(OBu^t)$_3$Hf]$_2$(μ-4DBP) (5). Used Hf(OBu^t)$_4$ (1.00 g, 2.12 mmol) and H$_2$-4DBP (0.451 g, 1.06 mmol). Yield: 1.81 g (69.9%). FTIR (KBr, cm^{-1}): 2969 (s), 2926 (m), 2869 (w), 1459 (w), 1424 (s), 1389 (w), 1361 (m), 1266 (s), 1233 (m), 1208 (s), 1188 (s), 1124 (m), 1053 (s), 1015 (s), 946 (w), 920 (w), 895 (w), 875 (m), 861 (m), 789 (m), 776 (w), 698 (w). ^{1}H NMR (400.1 MHz, tol-d$_8$) δ 7.26 (1.7H, s, [OC$_6$*H*$_2$(C(CH$_3$)$_3$)$_2$]$_2$CH$_2$), 4.00 (0.8H, s, [OC$_6$H$_2$(C(CH$_3$)$_3$)$_2$]$_2$C*H*$_2$), 1.54 (17.6H, s, [OC$_6$H$_2$(C(C*H*$_3$)$_3$)$_2$]$_2$CH$_2$), 1.31 (27.0H, s, OC(C*H*$_3$)$_3$). Anal. Calcd for C$_{53}$H$_{96}$Hf$_2$O$_8$ (%): C, 52.25; H, 7.94. Found: C, 51.83; H, 8.14.

2.2.5. [(py)$_2$(Et)Zn]$_2$(μ-4DBP)·py (6). To a solution of Zn(Et)$_2$ (4.04 mL, 4.04 mmol) in tol (~3 mL), H$_2$-4DBP (0.860 g, 2.02 mmol) was slowly added. After this time, a few drops of py were added with evolution of a gas. The reaction turned from a clear colorless solution to an orange color. After stirring for 12 h, no precipitate was observed and crystals were isolated by slow evaporation of the volatile portion of the reaction mixture. Yield: 1.75 g (46.9%). FTIR (KBr, cm^{-1}): 3088 (w), 3061 (m), 3002 (m), 2949 (s), 2906 (s,sh), 2857 (s), 2800 (w,sh), 1061 (m), 1485 (w), 1458 (s,sh), 1446 (s), 1415 (s), 1380 (w), 1260 (s), 1213 (s), 1150 (w), 1069 (m), 1038 (m), 1012 (w), 825 (w), 752 (w), 700 (s), 595 (w). ^{1}H NMR (400.1 MHz, py-d$_5$) δ 8.75 (C$_5$*H*$_5$), 7.59 (C$_5$*H*$_5$), 7.51 (2.2H, OC$_6$*H*$_2$(C(CH$_3$)$_3$)$_2$]$_2$CH$_2$), 7.23 (C$_5$*H*$_5$), 4.21 (1.0H, s, [OC$_6$H$_2$(C(CH$_3$)$_3$)$_2$]$_2$C*H*$_2$), 1.57 (18.1H, s, [OC$_6$H$_2$(C(C*H*$_3$)$_3$)$_2$]$_2$CH$_2$), 1.51 (3.0H, t, CH$_2$C*H*$_3$, J_{H-H} = 8.1 Hz), 0.75 (2.0H, q, C*H*$_2$CH$_3$, J_{H-H} = 4.0 Hz). Anal. Calcd for C$_{53}$H$_{72}$N$_4$O$_2$Zn$_2$ (%): C, 68.60; H, 7.82; N, 6.04. Found: C, 67.76; H, 7.85; N, 5.46.

2.2.6. [(THF)$_3$(Br)Mg]$_2$(μ-4DBP) (7). To a solution of (Mes)MgBr (2.30 mL, 2.30 mmol) in tol/THF (~3.5 mL), H$_2$-4DBP (0.488 g, 1.14 mmol) was slowly added. The reaction remained colorless. After stirring for 12 h, no precipitate was observed and crystals were isolated by slow evaporation of the volatile portion of the reaction mixture. Yield: 0.782 g (47.1%). FTIR (KBr, cm^{-1}): 3054 (w,sh), 2995 (m,sh), 2949 (s), 2905 (s), 2868 (s), 1603 (w), 1463 (s), 1426 (s), 1382 (w), 1355 (w), 1302 (s), 1262 (m), 1200 (w), 1019 (s), 916 (w), 864 (s), 731 (m), 697 (w), 467 (w). ^{1}H NMR (400.1 MHz, tol-d$_8$) δ 7.40 (1.8H, [OC$_6$*H*$_2$(C(CH$_3$)$_3$)$_2$]$_2$CH$_2$), 4.16 (0.95H, s, [OC$_6$H$_2$(C(CH$_3$)$_3$)$_2$]$_2$C*H*$_2$), 3.61(12.7H, mult, OC$_4$H$_8$), 1.61 (18.0, s, [OC$_6$H$_2$(C(C*H*$_3$)$_3$)$_2$]$_2$CH$_2$), 1.51 (3.0H, t, CH$_2$C*H*$_3$, J_{H-H} = 8.1 Hz), 1.32 (12.8 H, mult, OC$_4$H$_8$). Anal. Calcd for C$_{45}$H$_{74}$Br$_2$Mg$_2$O$_6$ (%): C, 58.72; H, 8.11. Found: C, 58.02; H, 8.61.

2.3. *AlR$_3$ general synthesis*

To a stirring mixture of the desired AlR$_3$ in toluene, H$_2$-4DBP was slowly added. Effervescence was noted for each reaction and after this subsided a few drops of pyridine were added, which also led to the evolution of a small amount of gas. The color

changed from a clear to pale yellow. After stirring for 12 h, the reaction mixture was set aside to allow the volatile portion of the reaction mixture to slowly evaporate until X-ray quality crystals formed.

2.3.1. [(py)$(CH_3)_2$Al]$_2$(μ-4DBP) (8). Used $AlMe_3$ (0.500 g, 6.94 mmol) and H_2-4DBP (1.47 g, 3.47 mmol). Yield: 0.600 g (12.4%). FTIR (KBr, cm^{-1}): 3058 (w), 3022 (w), 2998 (w), 2954 (s), 2920 (s,sh), 2868 (s), 2705 (w), 1615 (m), 1491 (w), 1482 (w), 1462 (m), 1450 (s), 1423 (s), 1286 (s), 1273 (s,sh), 1218 (m), 1195 (m), 1157 (w), 1124 (w), 1070 (m), 1051 (m), 1019 (w), 900 (m,sh), 885 (s), 779 (w), 759 (w), 703 (s), 671 (s), 648 (m), 434 (w). ^{1}H NMR (400.1 MHz, py-d_5) δ 8.73 (C_5H_5), 7.57 (C_5H_5), 7.45 (2.0H, [$OC_6H_2(C(CH_3)_3)_2]_2CH_2$), 7.20 ($C_5H_5$), 4.10 (1.1H, s, [$OC_6H_2(C(CH_3)_3)_2]_2CH_2$), 1.45 (19.5H, s, [$OC_6H_2(C(CH_3)_3)_2]_2CH_2$), −0.18 (6.0H, s, CH_3). Anal. Calcd for $C_{43}H_{64}Al_2N_2O_2$ (%): C, 74.32; H, 9.28; N, 4.03. Found: C, 72.23; H, 9.03; N, 3.65.

2.3.2. [(py)$(Et)_2$Al]$_2$(μ-4DBP) (9). Used $AlEt_3$ (0.500 g, 4.38 mmol) and H_2-4DBP (0.931 g, 2.19 mmol). Yield: 0.712 g (21.3%). FTIR (KBr, cm^{-1}): 3067 (w), 3020 (w), 2955 (s), 2895 (s,sh), 2860 (s), 2797 (w), 2723 (w), 1615 (m), 1491 (m), 1483 (m,sh), 1450 (s), 1422 (s), 1387 (m), 1357 (m), 1283 (s), 1267 (s), 1215 (s), 1197 (m), 1158 (w), 1123 (w), 1070 (s), 1052 (m), 1020 (m), 977 (m,sh), 873 (s), 699 (m), 632 (m). ^{1}H NMR (400.1 MHz, py-d_5) δ 8.75 (C_5H_5), 7.60 (C_5H_5), 7.42 (2.0H, $OC_6H_2(C(CH_3)_3)_2]_2CH_2$), 7.23 ($C_5H_5$), 4.09 (1.0H, s, [$OC_6H_2(C(CH_3)_3)_2]_2CH_2$), 1.43 (17.8H, s, [$OC_6H_2(C(CH_3)_3)_2]_2CH_2$), 1.16 (5.0H, t, CH_2CH_3, $J_{H-H} = 8.2$ Hz), 0.52 (3.7 H, q, CH_2CH_3, $J_{H-H} = 8.1$ Hz). Anal. Calcd for $C_{47}H_{72}Al_2N_2O_2$ (%): C, 75.16; H, 9.66; N, 3.73. Found: C, 72.42; H, 9.49; N, 3.92.

2.3.3. [(py)$((CH_3)_2CHCH_2)_2$Al]$_2$(μ-4DBP) (10). Used $Al(Bu^i)_3$ (0.500 g, 2.52 mmol) and H_2-4DBP (0.535 g, 1.26 mmol). Yield: 0.672 g (30.8%). FTIR (KBr, cm^{-1}): 3071 (w), 3058 (w), 3019 (m), 2948 (s), 2918 (s,sh), 2886 (s,sh), 2862 (s), 2787 (w), 1613 (s), 1461(s), 1448 (s), 1421 (s), 1388 (s), 1359 (s), 1265 (s), 1215 (s), 1186 (m), 1159 (m), 1123 (m), 1068 (s), 1050 (s), 1017 (s), 941 (w), 899 (m), 871 (s), 818 (w), 781 (w), 762 (m), 702 (s), 667 (s), 647 (s), 439 (w). ^{1}H NMR (400.1 MHz, py-d_5) δ 8.75 (C_5H_5), 7.63 (C_5H_5), 7.36 (2.0H, [$OC_6H_2(C(CH_3)_3)_2]_2CH_2$), 7.30 ($C_5H_5$), 4.04 (0.9H, s, [$OC_6H_2(C(CH_3)_3)_2]_2CH_2$), 1.88 (1.8H, sept, $CH_2CH(CH_3)_2$, $J_{H-H} = 6.5$ Hz), 1.42 (18.4H, s, [$OC_6H_2(C(CH_3)_3)_2]_2CH_2$), 1.03 (12.0H, d, $CH_2CH(CH_3)_2$, $J_{H-H} = 3.2$ Hz), 0.66 (4H, d, $CH_2CH(CH_3)_2$, $J_{H-H} = 2.9$ Hz). Anal. Calcd for $C_{55}H_{88}Al_2N_2O_2$ (%): C, 76.52; H, 10.27; N, 3.25. Found: C, 75.68; H, 10.20; N, 4.41.

2.4. *General X-ray crystal structure information [25]*

Crystals were mounted onto a glass fiber from a pool of Fluorolube™ and immediately placed in a cold N_2 vapor stream on a Bruker AXS diffractometer equipped with a SMART 1000 CCD detector using graphite monochromated Mo-Kα radiation ($\lambda = 0.7107$ Å). Lattice determination and data collection were carried out using SMART Version 5.054 software. Data reduction was performed using SAINTPLUS Version 6.01 software and corrected for absorption using the SADABS program within the SAINT software package.

Structures were solved by direct methods that yielded the heavy atoms, along with a number of the lighter atoms or by using the PATTERSON method, which yielded the heavy atoms. Subsequent Fourier syntheses yielded the remaining light-atom positions. Hydrogen atoms were fixed in positions of ideal geometry and refined using APEX II software suite software. The final refinement of each compound included anisotropic thermal parameters for all non-hydrogen atoms. Crystal structures of $M(OR)_x$ often contain disorder within the atoms of the ligand chain causing higher than normal final correlations [4, 5, 26–29].

Data collection parameters for **1**–**10** are given in table 1. Metrical data are tabulated in table 2. Specific issues associated with individual structures follow. Slight ligand disorder in the pendant chains was present in **2**, **3**, **4**, **5**, **5a**, **7a**, and **10**. Attempts to resolve this disorder was done by applying standard crystallographic restraints using split occupancy with residual Q-peaks. For the most part this allowed the structures to refine to completeness and lowered the refinement values. Disordered solvent molecules were squeezed out using the PLATON squeeze method for **4**, **6**, **9**, and **10**.

3. Results and discussion

A large number of *ortho*-linked Group 4 bis-phenoxide structures are available in the literature where the ligand acts in a chelating manner due to the orientation of the hydroxides. This arrangement is abundant for calixarene derivatives, but this family of compounds is beyond the scope of this report. However, for three titanium chloro derivatives with the respective 2,2′-methylenebis(6-phenylphenoxy) [30] and 2,7-di-*t*-butyl-9H-fluororene-1,8-diolato-O,O) [31] the ligand acted as a bridge between two disparate metal centers. In addition, the Zr cyclopentatidenyl, chloro derivative possessed a 3-bromo-5,5′-di-*t*-butyl-2,2′oxydiphenylmethane bridge [32]. Again, these are not *para*-substituted and not alkoxide species, so comparisons may not be representative of the behavior of alkoxy or alkyl 4DBP derivatives. There are no reports of 4DBP derivatives for any transition metal complexes. Only two transition metals have been reported with even the basic connectivity of this type of ligand including $(Cp^*Ti)_2(\mu\text{-}4MPhO)_3$, where 4MPhO = 2,2′-bis(4-oxyphenyl)propane) [33], and $[(HB(DMP)_3)Mo(NO)(\mu\text{-}4MPhO)]_2$, where $HB(DMP)_3$ = hydrogen-tris-(3,5-dimethyl-pyrazol-1-yl)borate [34]. Therefore, the coordination behavior of the H_2-4DBP ligand was investigated through the reaction with sets of $M(OR)_x$ and MR_x.

The H_2-4DBP ligand (figures 1d and 2) was of interest for several reasons: (i) the *ortho* position possesses the sterically hindering *t*-butyl group which will assist in minimizing oligomerization, (ii) the *para* linkage prevents chelation of the 4DBP ligand to the metal upon coordination, and (iii) may act as a useful model for complexation behavior of the plastic precursor bisphenol-A [BPA; 4,4′-(propane-2,2-diyl)diphenol] that has become of recent concern [35]. The ligand itself (**1**) was isolated from pyridine and is shown in figure 2. As can be observed, the *para* position of the –OH moieties are not closely associated with each other with a bend of the Ar–CH_2–Ar angle of 115.4°. This arrangement should allow for ready substitution on both reactive –OH sites, which could lend some control.

Table 1. Data collection parameters for **1**–**10**.

Compound	**1**	**2**	**3**	**4**	**5**	**5a**
Chemical formula	$C_{29}H_{44}O_2$	$C_{106}H_{192}O_{16}Ti_4$	$C_{59}H_{108}O_8Ti_2$	$C_{53}H_{96}O_8Zr_2$	$C_{53}H_{96}Hf_2O_8$	$C_{63}H_{106}Hf_2N_2O_8$
Formula weight	424.64	1914.47	1041.25	1043.74	1218.30	1376.50
Temperature (K)	173(2)	173(2)	173(2)	173(2)	188(2)	173(2)
Crystal system	Tetragonal	Monoclinic	Monoclinic	Triclinic	Monoclinic	Monoclinic
Space group	*I4(1)/a*	*P2(1)/c*	*Cc*	$P-1$	*P2(1)/c*	*P2(1)/c*
Unit cell dimensions (Å, °)						
a	21.016(4)	18.488(2)	14.827(3)	10.760(4)	18.747(4)	20.998(3)
b	21.016(4)	19.638(2)	12.509(3)	16.978(5)	19.964(4)	17.794(2)
c	23.680(8)	16.435(2)	35.282(6)	18.890(6)	16.554(3)	40.654(5)
α				110.871(10)		
β		93.001(2)	94.216(5)	93.984(6)	93.356(2)	93.989(2)
γ				101.342(9)		
Volume (Å^3), *Z*	10,459(5), 16	5959.0(12), 2	6526(2), 4	3124.6(18), 2	6185(2), 4	15,154(3), 4
Calculated density (Mg m^{-3})	1.079	1.060	1.060	1.109	1.307	1.276
Absorption coefficient (Mo-Kα) (mm^{-1})	0.065	0.312	0.290	0.376	3.397	2.786
R_1[a] (%) (all data)	9.31 (12.98)	6.85 (11.26)	11.49 (20.03)	7.67 (16.78)	3.94 (4.88)	4.55 (7.23)
wR_2[b] (%) (all data)	25.53 (28.96)	18.84 (23.52)	27.45 (34.06)	17.36 (19.79)	11.53 (12.68)	10.43 (11.89)

Compound	**6**	**7**	**7a**	**8**	**9**	**10**
Chemical formula	$C_{53}H_{72}N_4O_2Zn_2$	$C_{49}H_{106}Br_2Mg_2O_8$	$C_{104}H_{164}Br_4Mg_4O_{12}$	$C_{43}H_{64}Al_2N_2O_2$	$C_{47}H_{72}Al_2N_2O_2$	$C_{55}H_{88}Al_2N_2O_2$
Formula weight	927.89	1031.78	2023.23	694.92	751.03	863.23
Temperature (K)	188(2)	173(2)	188(2)	173(2)	188(2)	188(2)
Crystal system	Monoclinic	Monoclinic	Monoclinic	Monoclinic	Orthorhombic	Orthorhombic
Space group	*P2(1)/c*	*P2(1)*	*P2(1)/n*	*P2(1)/c*	*Pbca*	*Pbca*
Unit cell dimensions (Å, °)						
a	18.5175(19)	9.3436(5)	18.0993(13)	11.068(3)	13.046(2)	14.3007(13)
b	14.4237(15)	17.1226(8)	16.5797(12)	20.625(6)	20.506(3)	25.699(2)
c	22.218(2)	18.3482(9)	19.4237(14)	18.551(5)	37.203(6)	33.405(3)
β	113.7820(10)	102.324(2)	110.9380(10)	90.640(6)		
Volume (Å^3), *Z*	5430.4(10), 4	2867.8(2), 2	5443.8(7), 2	4234(2), 4	9953(3), 8	12277(2), 8
Calculated density (Mg m^{-3})	1.135	1.232	1.234	1.090	1.002	0.934
Absorption coefficient (Mo-Kα) (mm^{-1})	0.922	1.482	1.556	0.104	0.092	0.081
R_1[a] (%) (all data)	4.72 (7.86)	6.19 (7.77)	4.68 (6.54)	8.08 (19.80)	7.51 (17.85)	7.12 (14.38)
wR_2[b] (%) (all data)	12.82 (15.59)	16.43 (17.54)	14.03 (15.30)	16.54 (22.72)	16.48 (21.38)	16.91 (20.14)

[a] $R_1 = \Sigma||F_o| - |F_c|| / \Sigma|F_o| \times 100$; [b] $wR_2 = [\Sigma w(F_o^2 - F_c^2)^2 / \Sigma(w|F_o|^2)^2]^{1/2} \times 100$.

Table 2. Bond distances (Å) and angles (°) for **1–10** (L = OR or R).

Compound	Metal	Distances (Å)		Angles (°)	
		$M–O_{Ar}$	M–L	Ar–CH_2–Ar	O_{Ar}–M–L
1	–	–	–	115.4	–
2	Ti	1.82	1.76	113.7	110.2
3	Ti	1.80	1.76	113.7	108.8
4	Zr	1.94	1.89	114.4	110.3
5	Hf	1.90	1.92	113.2	110.1
5a	Hf	1.99	1.92	112.9	112.8
6	Zn	1.93	1.99	116.1	129.1
7	Mg	1.83	2.41	113.5	119.8
7a	Mg	1.88	2.53	115.2	135.3
8	Al	1.95	1.74	113.5	117.1
9	Al	1.74	1.96	112.9	114.4
10	Al	1.74	1.97	113.3	111.0

3.1. *Alkoxides*

Our initial investigation focused on determining the coordination behavior of the 4DBP ligand with $M(OR)_x$. The OBu^t and ONep ligands were chosen for Group 4 metals, while the OEt or OEt/ONep species were used for Group 5 cations due to their availability, our experience with these compounds [36–39], the steric hindrance imparted by the existing ligand sets, and their ability to readily form crystals.

For each sample simple mixing of 4DBP with the desired $M(OR)_4$ was undertaken in toluene, as in equation (1). Upon mixing, each reaction turned from a clear solution to a bright yellow color, independent of the stoichiometry investigated. For the Zr reactions, a precipitate typically occurred which was easily redissolved upon slight warming. Crystals were isolated by allowing the reaction to cool to room temperature, followed by slow evaporation if necessary. The FTIR data clearly revealed that an exchange occurred for each reaction based on the absence of the –OH stretch from the 4DBP ligands with new M–O bends present in the fingerprint region. However, additional information as to the exact nature of the final product was needed and single-crystal X-ray studies were undertaken to aid in this endeavor.

For **2** and **3**, the reaction proceeded as written in equation (1) yielding "$Ti(OBu^t)_3$" or "$Ti(ONep)_3$," respectively, substitution on both –OH oxygen atoms of the 4DBP ligand. All efforts to isolate a monosubstituted product were not successful. Attempts with the heavier congeners led to the isolation of **4** and **5**, which have similar structures as noted for **1**. The structures of **2**–**5** are shown in figures 3–6, respectively. The compounds all have tetrahedrally (T_d) bound metal centers with an average bend angle of 113.6 noted for the $–CH_2$ aryl group linker. Furthermore, crystallization of **5** from pyridine led to coordination of a solvent molecule, yielding **5a** (figure 7). This compound possesses a coordinated py to the metal center and thus square base-pyramidal geometry ($\tau = 0.32$) with a bend angle of 112.9°. The remainder of the distances is in line with **1**–**5** (table 2) or literature values of similar compounds [30–34].

Interestingly, dinuclear $M(OR)_x$ appears to be unreactive toward substitution on the 4DBP ligand. For instance, a reaction of the dimeric Group 4 compounds [H][$M_2(\mu$-$ONep)_3(ONep)_5(OBu^t)$] [39] (M = Zr, Hf) heated at reflux in toluene with H_2-4DBP

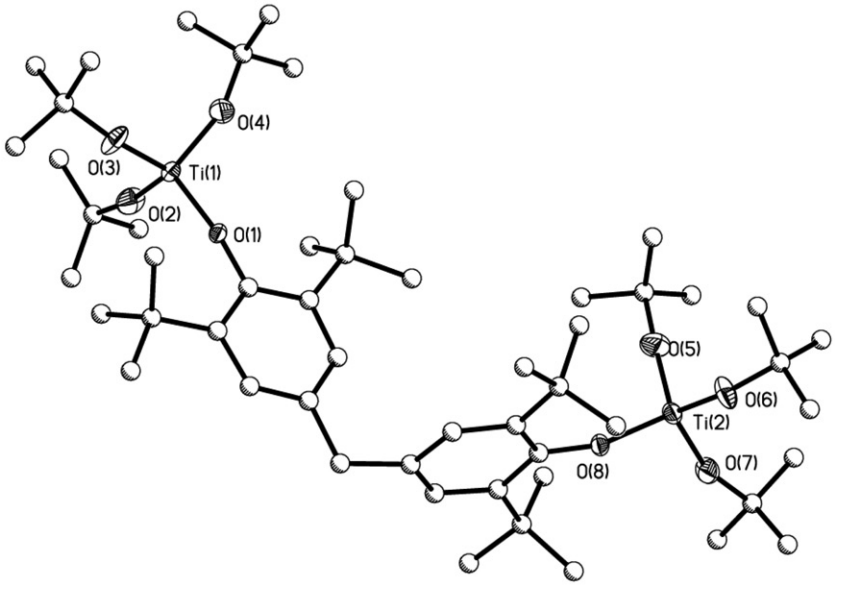

Figure 3. Structure plot of **2**. Heavy atom thermal ellipsoids drawn at 30% level and carbon atoms drawn as ball and stick for simplicity.

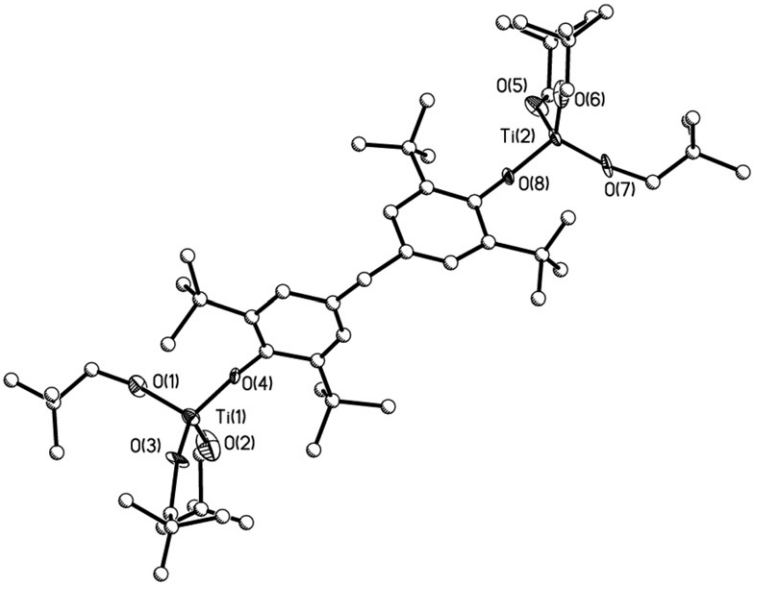

Figure 4. Structure plot of **3**. Heavy atom thermal ellipsoids drawn at 30% level and carbon atoms drawn as ball and stick for simplicity.

yielded only starting materials. Further, as Group 5 species were studied under similar conditions, it was noted that neither $[M(\mu\text{-}OEt)(OEt)_4]_2$ nor $[M(\mu\text{-}OEt)(ONep)_4]_2$ [36, 38] (where M = Nb, Ta) reacted with H_2-4DBP either. The dinuclear species are believed to be too sterically hindered to allow for the expected reaction (note: the solid

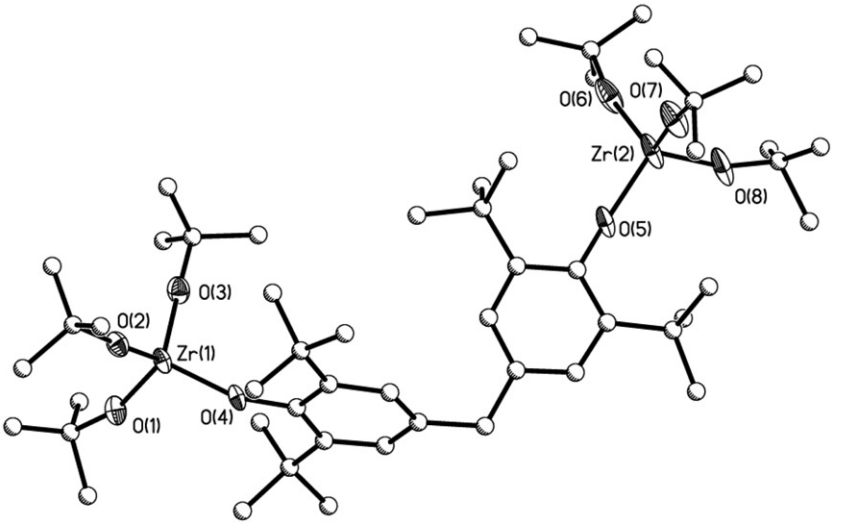

Figure 5. Structure plot of **4**. Heavy atom thermal ellipsoids drawn at 30% level and carbon atoms drawn as ball and stick for simplicity.

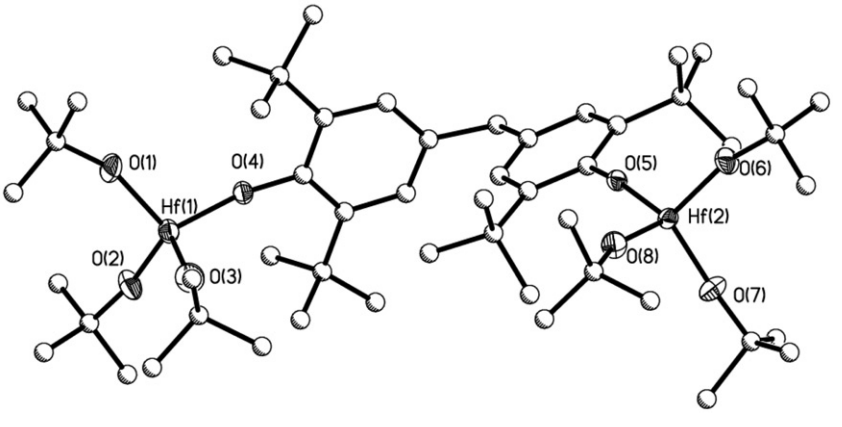

Figure 6. Structure plot of **5**. Heavy atom thermal ellipsoids drawn at 30% level and carbon atoms drawn as ball and stick for simplicity.

state structure of the dinuclear $[Ti(\mu\text{-}ONep)(ONep)_3]_2$ is reported to be monomeric in solution [37]).

3.2. *Alkyls*

Further investigation of the coordination behavior of H_2-4DBP was undertaken with a series of MR_x where the metal ranged from a late transition metal, to *s*-block to *p*-block metals.

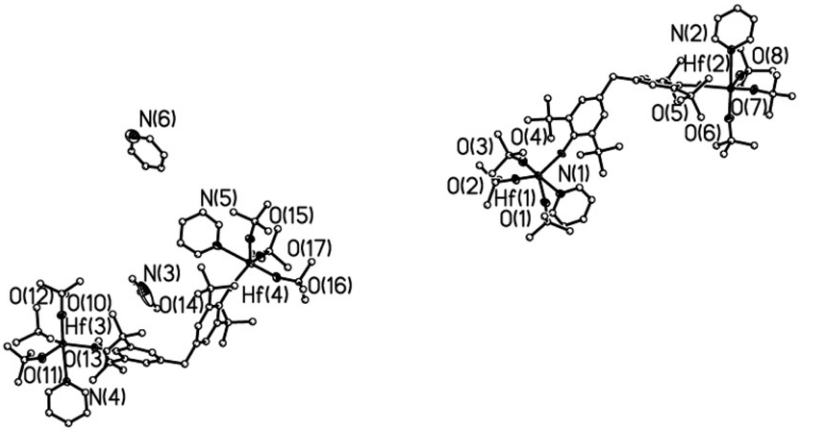

Figure 7. Structure plot of **5a**. Heavy atom thermal ellipsoids drawn at 30% level and carbon atoms drawn as ball and stick for simplicity. Two molecules were located in the unit cell.

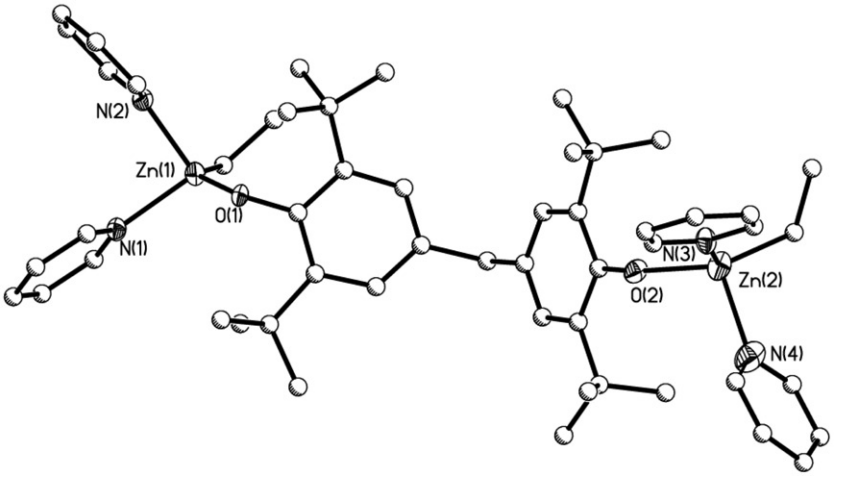

Figure 8. Structure plot of **6**. Heavy atom thermal ellipsoids drawn at 30% level and carbon atoms drawn as ball and stick for simplicity.

For the late transition metal, $ZnEt_2$ was modified by the 4DBP ligand according to equation (2). The resulting colorless solution required the addition of pyridine to grow X-ray quality crystals. FTIR data indicated the –OH had been removed and pyridine was present in the final material. For **6**, each –OH of the 4DBP ligand was successfully substituted by a "ZnEt" moiety. In addition, two molecules of py are bound to Zn to yield a T_d geometry (figure 8). The reaction of H_2-4DBP with (Mes)MgBr, where Mes = mesityl, led to isolation of an *s*-block metal derivative **7** (figure 9) from THF. The FTIR data were similar to that of **6**. Again, each –OH has been reacted liberating the H-Mes by product to form a di-Mg–Br substituted 4DBP derivative. Three THF molecules complete the distorted trigonal bipyramidal ($\tau = 0.70$) coordination sphere of

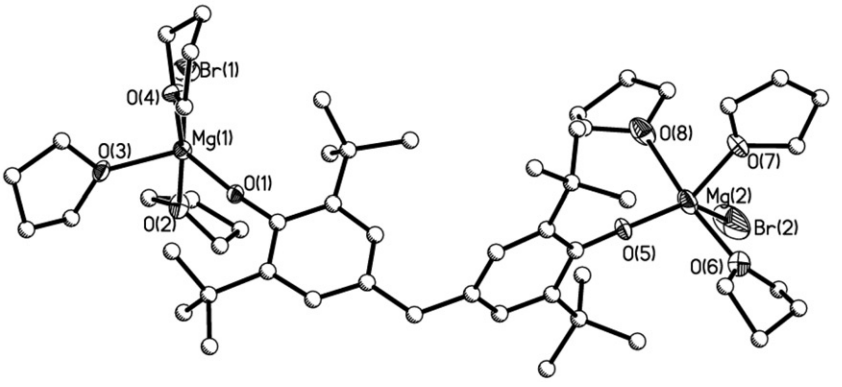

Figure 9. Structure plot of **7**. Heavy atom thermal ellipsoids drawn at 30% level and carbon atoms drawn as ball and stick for simplicity.

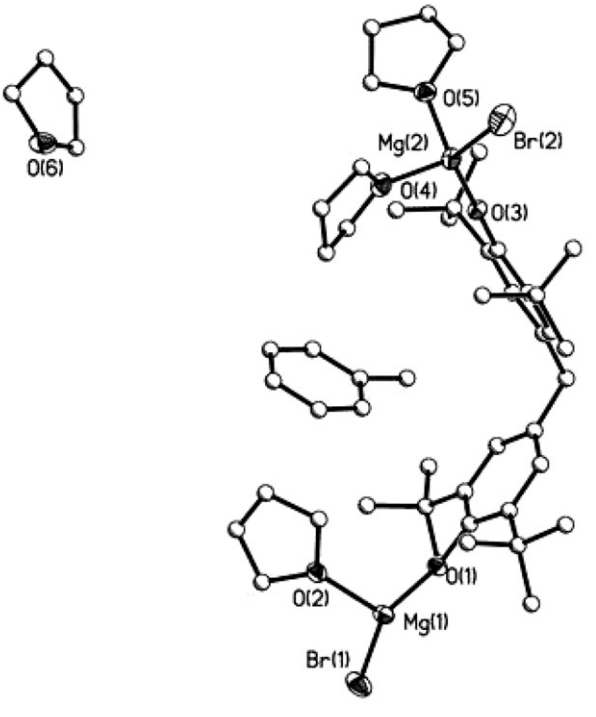

Figure 10. Structure plot of **7a** · THF,tol. Heavy atom thermal ellipsoids drawn at 30% level and carbon atoms drawn as ball and stick for simplicity.

the Mg. From a different crystallization attempt, an interesting alternative compound **7a** (figure 10) was isolated, where Mg(1) binds only one but Mg(2) binds two THF molecules. Additionally, a THF and a toluene molecule are located in the unit cell. This results in an asymmetrical molecule with one Mg adopting a distorted trigonal

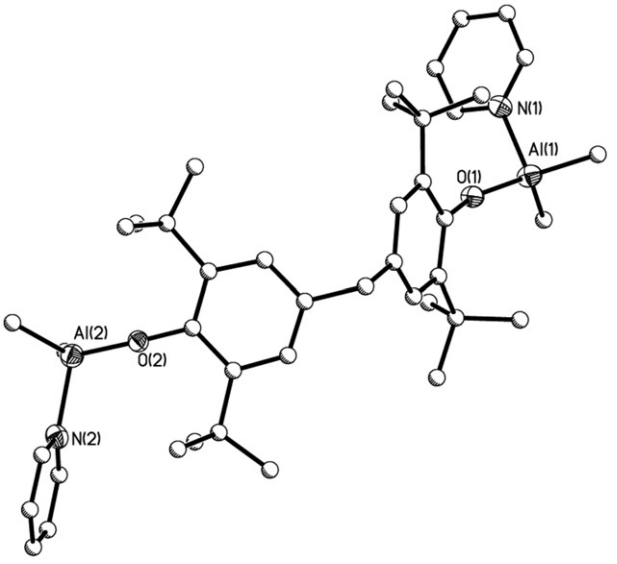

Figure 11. Structure plot of **8**. Heavy atom thermal ellipsoids drawn at 30% level and carbon atoms drawn as ball and stick for simplicity.

geometry and the other forming a T_d coordination. The Ar–CH_2–Ar bend angles for **6**–**7a** (table 2) were found to be consistent with each other and with **2**–**5a**.

Finally *p*-block main group Al was studied (equation (2)) using AlR_3 [where R=CH_3, CH_2CH_3, $CH_2CH(CH_3)_2$]. The reactions proceed as written, changing from colorless to pale yellow upon addition of 4DBP. Crystals were isolated from a pyridine solution and FTIR data collected on these compounds show the loss of –OH peak along with standard 4DBP stretches and bends. This suggests that the same substitution occurred and was confirmed by single-crystal studies. For **8**–**10**, similar di-substituted compounds (see figures 11–13, respectively) were noted with each Al metal center adopting a T_d geometry by binding a py along with its parent ligands and one O from 4DBP. The bond distances and angles of these similar species are in agreement (see table 2).

3.3. *Thermal analyses*

Elemental analyses of crystalline material proved to be inconsistent with the best values reported in section 2. For $M(OR)_x$ this is often attributed to solvent loss, volatilization, or decomposition of the precursor. However, the $M(OR)_4$ derivatives are close to the acceptable range, while the solvated species were not within the calculated values. Further analyses were undertaken to understand these variations.

Melting point determinations were undertaken for each compound from room temperature to 300°C. H_2-4DBP (**1**) was found to have a melting point of 155°C and as expected, upon complexation, the melting point changes [Cmpd (m.p. °C)]: **2** (185), **3** (185), **4** (110), **5** (120), **8** (220), **9** (220), **10** (120). Compounds **6** and **7** did not melt in this study. The lowering of the m.p. of **4**, **5**, and **10** below that of the ligand is an interesting effect that needs to be further explored. However, the melting point data indicate that

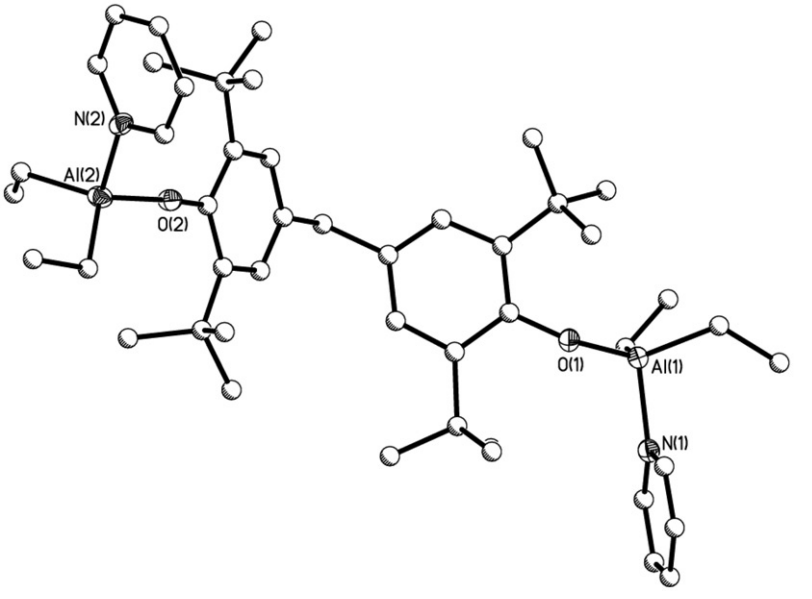

Figure 12. Structure plot of **9**. Heavy atom thermal ellipsoids drawn at 30% level and carbon atoms drawn as ball and stick for simplicity.

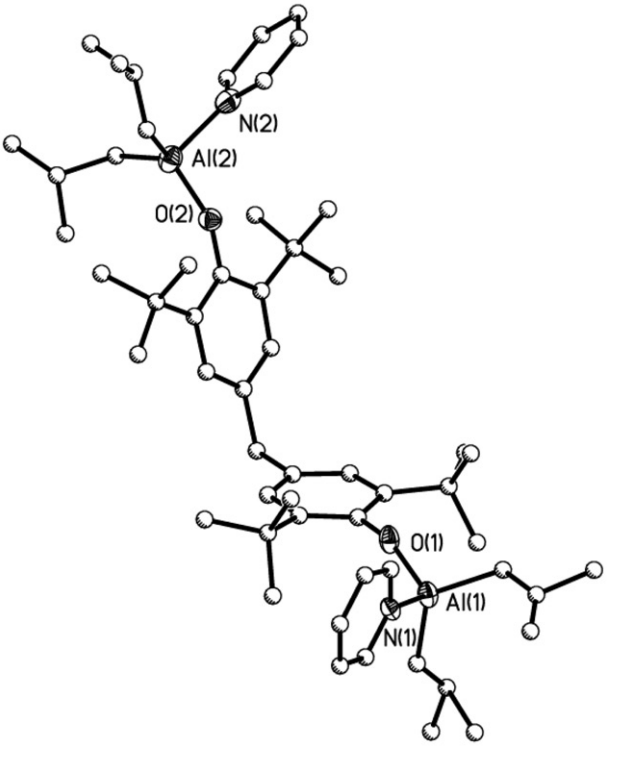

Figure 13. Structure plot of **10**. Heavy atom thermal ellipsoids drawn at 30% level and carbon atoms drawn as ball and stick for simplicity.

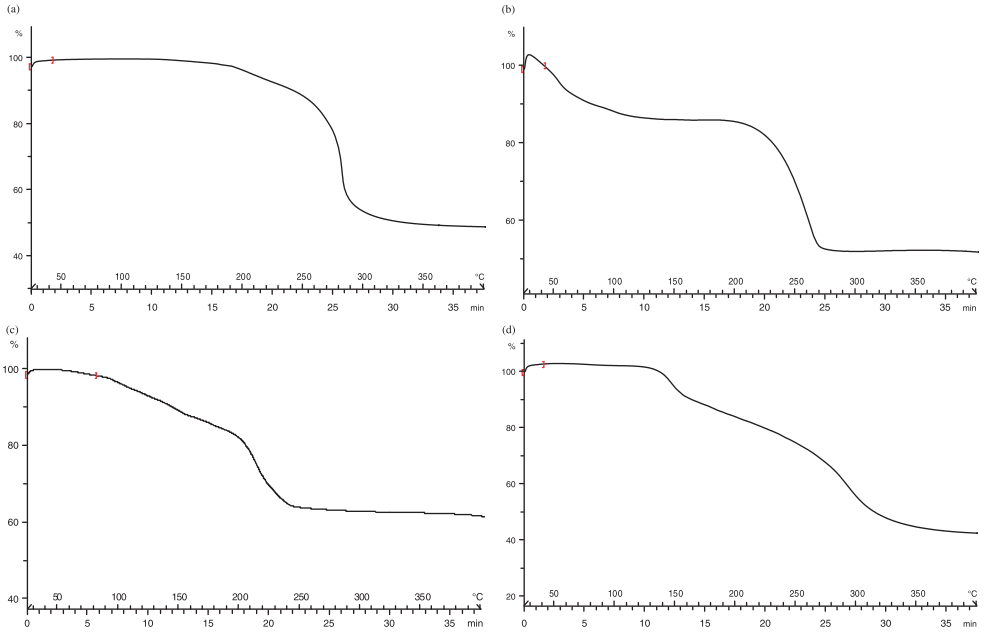

Figure 14. TGA data collected under argon (5°C min^{-1} to 400°C) for (a) **4**, (b), **6**, (c) **7**, and (d) **10**.

for a majority of these compounds, a preferential melt and volatilization probably occur prior to decomposition.

Further studies on the thermal behavior were undertaken using TGA analyses of representative species (i.e., **4**, **6**, **7**, and **10**). The weight loss associated with 4DBP was found to initiate around 200°C for each model compound. Figure 14 shows the TGA spectra up to 400°C of (a) **4**, (b), **6**, (c) **7**, and (d) **10**. For **4**, the early weight loss is consistent with loss of 4DBP along with some OBu^t (overall weight loss 51.4; −2 OBu^t, −4DBP = 51.1). For **6**, the experimental weight loss of −49.3% is consistent with loss of 4DBP (−45.6%) and some pyridine moieties. For **7**, the overall weight loss is consistent with loss of −4DBP (Calcd 41.0%; exp: 38.8%). For **10**, the calculated weight change of 50.6% based on loss of 4DBP was found to be consistent with experimental weight loss of 49.8% (the early weight loss was consistent with one py). Combined these data indicate that initiation of 4DBP loss (and other moieties necessary to maintain charge balance) occurs at the relatively low temperature of 200°C, making obtaining acceptable elemental analyses difficult.

Interestingly, the overall weight loss (under an argon atmosphere up to 800°C) was *not* consistent with formation of the simple oxide. Therefore, thermal treatments of the powders outside of the TGA instrument were performed and the resulting powders analyzed by PXRD. The final powders for (a) **4**, (b) **6**, (c) **7**, and (d) **10** were identified as: (a) mixed phase of baddeleyite (PDF: 00-050-1089)/zirconium oxide (PDF: 00-050-1089), (b) amorphous, (c) zincite (PDF: 00-005-0664), and (d) periclase (PDF: 00-004-0829), respectively. The thermal treatment used in these experiments formed the ceramic oxide but may not have fully converted all of the material, as evidenced by the surprising amorphous Al derivative. Based on the low temperature melting and

preferential 4DBP loss, **1**–**10** are being studied as optimal precursors for metal-organic chemical vapor deposition (MOCVD) and nanomaterial applications.

3.4. *Solution behavior*

To determine if the structures were retained in solution, crystals of **1**–**10** were individually dissolved in a deuterated solvent at as concentrated levels as possible. The spectra were collected at room temperature. For H_2-4DBP, a simple, spectrum with four singlets (OH, aromatic H, CH_2, and Bu^t in a 1 : 2 : 1 : 18) are expected and observed for the ^{1}H NMR. Based on the obtained structures, upon complexation to the metals, the symmetry should not be reduced and a similar pattern (with the loss of the –OH peak) along with the inclusion of the resonances associated with the respective pendant ligand chains is expected. For **1**, **3**, and **4** nearly identical ^{1}H spectra were collected with four peaks observed in a 2 : 1 : 18 : 27 ratio representing the 4DBP ligand and the OBu^t of the metal. For **2**, a similar spectrum as above but two ONep peaks replaced the OBu^t resonances. For **6**, **8**, **9**, and **10**, three peaks associated with the 4DBP ligand were recorded in the ^{1}H NMR spectrum along with the respective single set of peaks for the pendant alkyl chains of MR_x. Finally, for **7**, only the resonances associated with the ligand were noted, which was expected since the pendant ligand was Br; however, collecting this spectrum in toluene provided two additional THF resonances in an integration equivalent to three solvent molecules, which is in agreement with the crystal structure of **7**. Combined the solution data are consistent with retention of the symmetric substitution of 4DBP and argues for retention of the solid state structures for **1**–**10**.

4. Conclusion

The first example of $M(OR)_4$ and MR_x derivatized by 4DBP have been reported as **1**–**10**. The protons of the –OH moieties were easily replaced with monomeric species, allowing for general di-substituted (μ-4DBP) structures to be isolated. Solution state NMR indicates these compounds retain their structures in solution. Thermal decomposition studies show these compounds preferentially melt instead of combusting, an unusual behavior for metal alkoxides and alkyls. Additionally, TGA data indicate that the 4DBP ligands are preferentially lost during thermal heating. This may allow for their utility as a clean route to thin films of metal oxides (i.e., MOCVD processing). Additional work to generate mixed metal species and explore their utility for materials applications and as a model of bisphenol A [35] are underway.

Supplementary material

The crystal structures of **1**–**10** have been deposited at the Cambridge Crystallographic Data Centre and allocated the deposition numbers CCDC 845610–845621. All final CIF files were checked at http://www.iucr.org/. Additional information concerning the

data collection and final structural solutions can be found in the supplemental information or by accessing CIF files through the Cambridge Crystallographic Data Base.

Acknowledgments

The authors thank Mr B. Simmon (Sandia) for PXRD analyses, use of the Bruker X-ray diffractometer [National Science Foundation CRIF : MU award to the University of New Mexico (CHE04-43580)], the National Institute for NanoEngineering (NINE) program, and the Laboratory Directed Research and Development (LDRD) program for supporting this research. Sandia National Laboratories is a multi-program laboratory managed and operated by Sandia Corporation, a wholly owned subsidiary of Lockheed Martin Corporation, for the U.S. Department of Energy's National Nuclear Security Administration under contract DE-AC04-94AL85000.

References

[1] D.C. Bradley, R.C. Mehrotra, D.P. Gaul. *Metal Alkoxides*, Academic Press, New York (1978).
[2] D.C. Bradley, R.C. Mehrotra, A.P. Rothwell, A. Singh. *Alkoxo and Aryloxo of Metals*, Academic Press, San Diego (2001).
[3] K.G. Caulton, L.G. Hubert-Pfalzgraf. *Chem. Rev.*, **90**, 969 (1990).
[4] C.D. Chandler, C. Roger, M.J. Hampden-Smith. *Chem. Rev.*, **93**, 1205 (1993).
[5] L.G. Hubert-Pfalzgraf. *New J. Chem.*, **11**, 663 (1987).
[6] H. Gerung, T.J. Boyle, L.J. Tribby, S.D. Bunge, C.J. Brinker, S.M. Han. *J. Am. Chem. Soc.*, **128**, 5244 (2006).
[7] T.J. Boyle, L.A.M. Ottley, M.A. Rodriguez. *Polyhedron*, **24**, 1727 (2005).
[8] S.D. Bunge, K.M. Krueger, T.J. Boyle, M.A. Rodriguez, T.J. Headley, V.L. Colvin. *J. Mater. Chem.*, **13**, 1705 (2003).
[9] H. Gerung, S.D. Bunge, T.J. Boyle, C.J. Brinker, S.M. Han. *Chem. Commun.*, 1914 (2005).
[10] T.J. Boyle, B.A. Hernandez-Sanchez, C.M. Baros, L.N. Brewer, M.A. Rodriguez. *Chem. Mater.*, **19**, 2016 (2007).
[11] T.J. Boyle, L.A.M. Ottley, S.D. Daniel-Taylor, L.J. Tribby, S.D. Bunge, A.L. Costello, T.M. Alam, J.C. Gordon, T.M. McCleskey. *Inorg. Chem.*, **46**, 3705 (2007).
[12] T.J. Boyle, S.D. Bunge, T.M. Alam, G.P. Holland, T.J. Headley, G. Avilucea. *Inorg. Chem.*, **44**, 1309 (2005).
[13] B.A. Hernandez-Sanchez, T.J. Boyle, C.M. Baros, L.N. Brewer, T.J. Headley, D.R. Tallant, M.A. Rodriguez, B.A. Tuttle. *Chem. Mater.*, **19**, 1459 (2007).
[14] T.J. Boyle, M.A. Rodriguez, T.M. Alam. *Dalton Trans.*, 4598 (2003).
[15] T.J. Boyle, R.M. Sewell, L.A.M. Ottley, H.D. Pratt, C.J. Quintana, S.D. Bunge. *Inorg. Chem.*, **46**, 1825 (2007).
[16] T.J. Boyle, M.A. Rodriguez, D. Ingersoll, T.J. Headley, S.D. Bunge, D.M. Pedrotty, S.M. De'Angeli, S.C. Vick, H.Y. Fan. *Chem. Mater.*, **15**, 3903 (2003).
[17] T.J. Boyle, D.M. Pedrotty, T.M. Alam, S.C. Vick, M.A. Rodriguez. *Inorg. Chem.*, **39**, 5133 (2000).
[18] T.J. Boyle, S.D. Bunge, N.L. Andrews, L.E. Matzen, K. Sieg, M.A. Rodriguez, T.J. Headley. *Chem. Mater.*, **16**, 3279 (2004).
[19] S.D. Bunge, T.J. Boyle, H.D. Pratt, T.M. Alam, M.A. Rodriguez. *Inorg. Chem.*, **43**, 6035 (2004).
[20] T.J. Boyle, N.L. Andrews, M.A. Rodriguez, C. Campana, T. Yiu. *Inorg. Chem.*, **42**, 5357 (2003).
[21] T.J. Boyle, S.D. Bunge, P.G. Clem, J. Richardson, J.T. Dawley, L.A.M. Ottley, M.A. Rodriguez, B.A. Tuttle, G.R. Avilucea, R.G. Tissot. *Inorg. Chem.*, **44**, 1588 (2005).
[22] T.J. Boyle, L.J. Tribby, T.M. Alam, S.D. Bunge, G.P. Holland. *Polyhedron*, **24**, 1143 (2005).
[23] T.J. Boyle, L.A.M. Ottley. *Inorg. Chim. Acta*, **364**, 69 (2010).
[24] T.J. Boyle, T.M. Alam, E.R. Mechenbier, B.L. Scott, J.W. Ziller. *Inorg. Chem.*, **36**, 3293 (1997).

[25] T.J. Boyle, T.M. Alam, C.J. Tafoya, E.R. Mechenbier, J.W. Ziller. *Inorg. Chem.*, **38**, 2422 (1999).
[26] D.C. Bradley, R.C. Mehrotra, D.P. Gaur. *Metal Alkoxides*, Academic Press, New York (1978).
[27] D.C. Bradley, R.C. Mehrotra, I.P. Rothwell, A. Singh. *Alkoxo and Aryloxo Derivatives of Metals*, Academic Press, New York (2001).
[28] N.Y. Turova, E.P. Turevskaya, V.G. Kessler, M.I. Yanovskaya. *The Chemistry of Metal Alkoxide*, Kluwer Academic, Boston (2002).
[29] K.G. Caulton, L.G. Hubert-Pfalzgraf. *Chem. Rev.*, **90**, 969 (1990).
[30] D.R. Mulford, P.E. Fanwick, I.P. Rothwell. *Polyhedron*, **19**, 35 (2000).
[31] O. Saied, M. Simard, J.D. Wuest. *Inorg. Chem.*, **37**, 2620 (1998).
[32] U. Hagenau, J. Heck, W. Kaminsky, A.-M. Schauwienold. *Z. Anorg. Allg. Chem.*, **626**, 1814 (2000).
[33] Y.-L. Lyu, Y. Byun, J.-H. Yim, S. Chang, S.-Y. Lee, L.S. Pu, I.-M. Lee. *Eur. Polym. J.*, **40**, 1051 (2004).
[34] F.S. McQuillan, H. Chen, T.A. Hamor, C.J. Jones, H.A. Jones, R.P. Sidebotham. *Inorg. Chem.*, **38**, 1555 (1999).
[35] S.K. Ritter. *Chem. Eng. News*, **June 6, 2011**, 13 (2011).
[36] T.J. Boyle, J.J. Gallegos, D.M. Pedrotty, E.R. Mechenbier, B.L. Scott. *J. Coord. Chem.*, **47**, 155 (1999).
[37] T.J. Boyle, T.M. Alam, E.R. Mechenbier, B.L. Scott, J.W. Ziller. *Inorg. Chem.*, **36**, 3293 (1997).
[38] T.J. Boyle, T.M. Alam, D. Dimos, G.J. Moore, C.D. Buchheit, H.N. Al-Shareef, E.R. Mechenbier, B.R. Bear, J.W. Ziller. *Chem. Mater.*, **9**, 3187 (1997).
[39] T.J. Boyle, L.A.M. Ottley, S.M. Hoppe, C.F. Campana. *Inorg. Chem.*, **49**, 10798 (2010).